The Astrophysical Journal, 499:L5–L8, 1998 May 20


# RESOLVING THE STRUCTURE OF COLD DARK MATTER HALOS

B. Moore,[1] F. Governato,[1] T. Quinn,[2] J. Stadel,[2] and G. Lake[2]
*Received 1997 September 9; accepted 1998 March 23; published 1998 May 13*

## ABSTRACT

We examine the effects of mass resolution and force softening on the density profiles of cold dark matter halos that form within cosmological *N*-body simulations. As we increase the mass and force resolution, we resolve progenitor halos that collapse at higher redshifts and have very high densities. At our highest resolution we have nearly $3 \times 10^6$ particles within the virial radius, which is several orders of magnitude more than previously used, and we can resolve more than 1000 surviving dark matter halos within this single virialized system. The halo profiles become steeper in the central regions, and we may not have achieved convergence to a unique slope within the inner 10% of the virialized region. Results from two very high resolution halo simulations yield steep inner density profiles, $\rho(r) \sim r^{-1.4}$. The abundance and properties of arcs formed within this potential will be different from calculations based on lower resolution simulations. The kinematics of disks within such a steep potential may prove problematic for the cold dark matter model when compared with the observed properties of halos on galactic scales.

*Subject headings:* cosmology: theory — dark matter — galaxies: halos — galaxies: clusters: general — methods: numerical

## 1. INTRODUCTION

The cold dark matter (CDM) model is a highly successful and well-motivated cosmological model. The basic premises are an inflationary universe dominated by a dark matter particle, such as the axion, that leads to "bottom up" hierarchical structure formation. Small dense halos collapse at high redshifts and merge successively into the large virialized systems that contain the galaxies that we observe today (e.g., Davis et al. 1985 and references therein). The properties of dark matter halos in the CDM model have been extensively investigated by numerous researchers since the early 1980s. The first results of Quinn et al. (1986) and Frenk et al. (1988) did not have the resolution necessary to probe the "observed" region of dark halos but did show isothermal structures in the outer regions. Higher resolution simulations by Dubinski & Carlberg (1991), Warren et al. (1992), Carlberg (1994), and Crone, Evrard, & Richstone (1994) showed evidence for density profiles with slopes flatter than isothermal in the central regions, with densities varying as $r^{-1}$ in the inner 10% of the halos. Navarro, Frenk, & White (1996, hereafter NFW) found that the density profiles of halos follow a universal form which is uniquely determined by their mass and virial radius, with values that vary from $r^{-1}$ in the central regions and smoothly roll over to $r^{-3}$ at the virial radii. (The virial radius $r_{\rm vir}$ is defined as the radius of a sphere containing a mean mass overdensity of 200 with respect to the global value). The NFW halos typically contained $\lesssim$10,000 particles, a number that was claimed to be sufficient to resolve the density profile of halos beyond a distance ~1% of the virial radius.

In this paper, we investigate the inner structure of CDM halos using *N*-body simulations with much higher mass and force resolution than used previously. We shall test separately the effects of softening and particle number on the final density profiles and the issue of convergence to a unique profile. Similar tests were performed by Tormen, Bouchet, & White (1996) and Craig (1997). Although the scale of their tests was smaller than that of the tests carried out here, their results suggested a similar dependence on numerical resolution. We begin with a brief discussion of the numerical techniques and simulation parameters. In § 3 we show visually and graphically how the structure and substructure of dark halos changes with numerical resolution, and we attempt to separate the effects of force softening and mass resolution on the density profiles. Finally, we discuss the role of resolution in determining halo density profiles and possible origins of the steep inner density cusps.

## 2. TECHNIQUES AND INITIAL CONDITIONS

Simulating the formation of a dark matter halo requires an accurate treatment of the cosmological tidal field from a large volume of the universe while obtaining high resolution throughout the infall and turnaround regions that will constitute the final halo. A candidate halo is initially identified from a large cosmological volume that has been simulated at lower resolution. The particles within the selected halo are traced back to the initial conditions to identify the region that will be resimulated at higher resolution. The power spectrum is extrapolated down to smaller scales, matched at the boundaries in such a way that both the power and the waves of the new density field are identical in the region of overlap, and then this region is populated with a new subset of less massive particles. Beyond the high-resolution region, the mass resolution is decreased in a series of shells such that the external tidal field is modeled correctly in a cosmological context.

The particle distribution is evolved using a new high-performance parallel tree code, PKDGRAV, which has accurate periodic boundaries (previous studies using tree codes had vacuum boundary conditions) and a variable time step criterion based upon the local acceleration. The code uses a comoving spline softening length such that the force is completely Newtonian at twice our quoted softening lengths. In terms of the point at which the force is 50% of the Newtonian force, the equivalent Plummer softening length would be 0.67 times the spline softening length. PKDGRAV has been extensively tested using a variety of methods—for example, comparing forces with those calculated using a direct $N^2$ code on a clustered particle distribution or comparing the growth of waves against

[1] Department of Physics, University of Durham, Durham City, DH1 3LE, England, UK.
[2] Department of Astronomy, University of Washington, Seattle, WA 98195.

linear predictions. We also find excellent agreement between PKDGRAV and the results of a particle-particle–particle mesh simulation of the "cluster comparison halo" using $10^6$ particles (Frenk et al. 1998).

We resimulate two halos that are both extracted from standard CDM simulations normalized such that $\sigma_8 = 0.7$ and the shape parameter $T = 0.5$ ($H = 50$ km s$^{-1}$ Mpc$^{-1}$ is adopted throughout). The "Virgo" halo has a virial radius of 2 Mpc and was extracted from an initial simulation with a box length of 100 Mpc. The "Coma" halo has a virial radius of 3.4 Mpc and was extracted from a larger initial simulation that had a volume of 1 Gpc$^3$. We performed several simulations of each halo; at our highest resolution, the particle mass in the highest resolution regions was $8 \times 10^8\ M_\odot$, and we used a 5 kpc softening length.

## 3. RESULTS

Figure 1 (Plate L1) shows the final density distribution of our highest resolution simulation of the Coma Cluster. The left-hand panel shows almost all of the 1000 Mpc box and illustrates the nested refinement zones, although when plotted on this scale, the central cluster is not resolved. In the right-hand panel, we have extracted a sphere of radius 3.4 Mpc $= r_{\rm vir}$ around the cluster. A wealth of substructure and "halos within halos" can be seen within this cluster. Figure 2 (Plate L2) shows the physical densities (*left*) and the phase-space densities (*right*) of the Coma halo simulated at three different resolutions. The upper plot shows the cluster simulated at a resolution similar to that used by NFW. There are about 13,000 particles within the virial region. The middle and lower plots show the same cluster simulated at higher resolution such that there are $1 \times 10^5$ and $2.7 \times 10^6$ particles, respectively, within the virial radius. The visual difference is remarkable. As we increase the mass resolution, we begin to resolve more and more substructure; at the highest resolution, there are ~1500 halos within $r_{\rm vir}$. A detailed analysis of the properties and dynamics of the dark matter substructure within the Virgo Cluster simulation can be found in Ghigna et al. (1998).[3]

In Figure 3 we show the density profile (calculated in spherical shells) of the Coma Cluster simulated with different mass and force resolutions. The halo centers are identified both using the center of mass of the inner halo and using the most bound particle, and the two methods give very similar results. We find that at higher resolutions, the central halo density profiles become steeper, and as we increase the mass resolution by a factor of 200, the density at 1% of the virial radius increases by 250%.

We have performed five simulations of this cluster in which we systematically increased the mass resolution such that we have a total of 92, 1450, 13,000, 100,000, and 2,700,000 particles within $r_{\rm vir}$. In each simulation, we set the softening parameter to be 1/50 of the mean interparticle separation in the highest resolution region; in the highest resolution run, the softening was equal to 5 kpc. For each simulation, we determine the radius at which the density profile falls by 20% with respect to the highest resolution simulation and define this to be a "reliable" radius beyond which we can trust the results. We find that this radius decreases systematically from 13% to 4.5%, 2.8%, and 1.9% of $r_{\rm vir}$, and the total numbers of particles that lie within these radii are 9, 35, 160, and 700, respectively. We conclude from this experiment that setting a minimum particle number is an insufficient criterion for defining the radius outside of which to "believe" the density profile. In fact, the reliable radius defined in this way is very close to a scale equal to 0.5 times the mean interparticle separation of those particles within $r_{\rm vir}$.

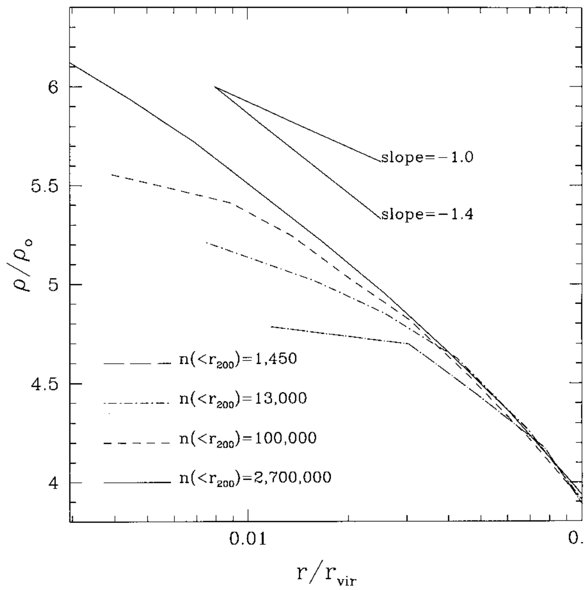


FIG. 3.—Density profiles of the Coma Cluster simulated at four different resolutions. The curves begin at the spline softening lengths that were used, and the number of particles within the final virial radii is indicated.

These convergence tests show that a factor of 8 in mass resolution leads to a factor of 4 increase in the number of particles needed to define the reliable radius. We therefore estimate that the highest resolution run is correct to a radius that contains about 5600 particles, which is 0.8% of $r_{\rm vir}$. At this point, the slope of the density profile has converged to a value of $r^{-1.4}$. It is possible that further increases in resolution will trace out this asymptotic gradient to higher densities but not to significantly steeper slopes.

### 3.1. *Force Softening and Particle Number*

We are attempting to model a collisionless system by sampling phase space with a small number of particles. This sampling introduces numerical noise that is ameliorated by softening the gravitational force on small scales that can affect the halo properties. The number of particles defines the smallest halo that can collapse at high redshifts and thus introduces a maximum phase-space density that can be resolved. The effect of softening is to introduce a "soft" core at the centers of all the halos approximately the size of the softening length. This causes halos to be disrupted more easily from tidal forces—the mechanism responsible for the overmerging problem (Moore et al. 1996).

At a fixed mass resolution, decreasing the softening will lead to higher central densities, but there will be a point at which smaller softening lengths will not change the inner profile. At this point, the density profile turns over to a constant value that is set by the maximum density that can be resolved by the first collapsing halos—unless artificial relaxation occurs. Figure 4 shows the effects of softening on the Virgo Cluster profile. This halo has ~20,000 particles within the virial radius of 2

[3] We note that the inner 10% of even the highest resolution cluster is entirely smooth. The overmerging problem is still inherent in dark matter simulations as a result of halo-halo collisions and the global tidal field destroying halos that pass close to the center (Moore, Katz, & Lake 1996).

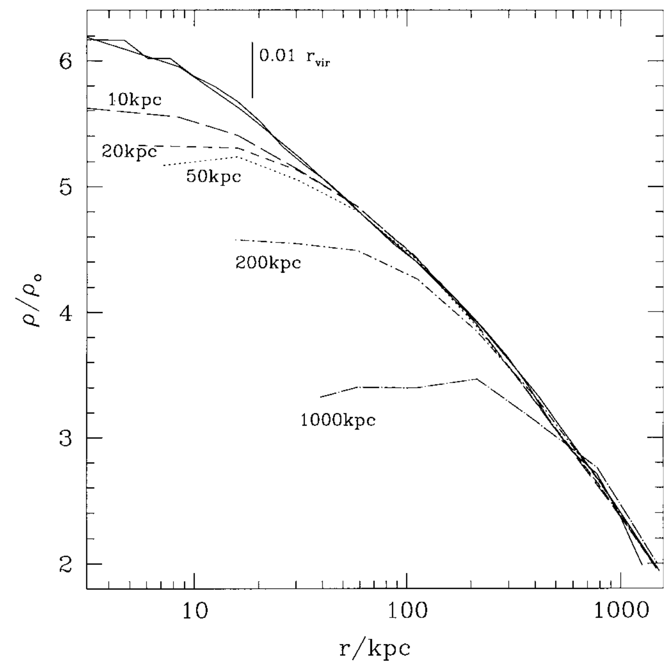


FIG. 4.—Long-dashed, dashed, dotted, dash-dotted, and long-dash–dotted lines show the Virgo halo simulated at the same mass resolution but varying only the softening parameter. This halo has a virial radius of 2 Mpc and contains 20,000 particles within $r_{\rm vir}$. The values of the softening used are indicated next to each curve. The solid curves show the same cluster resimulated with a mass resolution 20 times higher but keeping the force softening fixed at 10 kpc. To demonstrate that relaxation is not affecting our results, one of the solid curves shows the profile at a redshift $z = 0.25$.

Mpc, and we simulate it using values of the softening length ranging from 1 kpc to 1 Mpc. The density profiles are plotted on scales smaller than the adopted softening lengths to indicate the behavior in the inner regions, but results on scales less than the softening length have no physical meaning. Having said this, we note how well the density profile agrees on all scales slightly larger than the softening length. As the softening length is decreased, we converge upon the same profile found by NFW with a slope tending toward $r^{-1}$ in the inner regions. Eventually we run out of particles to resolve the inner regions, and decreasing the softening from 20 to 10 kpc has very little effect on the halo profile.[4]

The solid lines in Figure 4 show the same cluster simulated with 10 kpc softening but with 20 times as many particles. This leads to a significantly steeper density profile than the same halo simulated with the same softening but using fewer particles. At a radius equal to 1% of the virial radius, which is just over two softening lengths, the density increases by 70%. Within this radius, the low-resolution run contains over 50 particles. The two solid lines in Figure 4 show the density profiles of the same halo at redshifts $z = 0$ and $z = 0.25$ several billion years before the final output. This halo contains almost half a million particles within the virial radius, and over 90% of the mass is in place at a redshift $z = 0.25$. The density profiles normalized to $r_{\rm vir}$ are almost identical at the two epochs, which demonstrates that relaxation at late times or other numerical artifacts are not affecting our results even in the central regions.

Although a great deal of substructure is evident in these simulations, the bulk of the mass distribution in these halos lies within a smooth background of particles that were tidally stripped from the infalling halos. A single subclump with velocity dispersion $\sigma_{\rm sub}$ will introduce a fluctuation in the density profile of $\delta\rho/\rho \sim \delta M_{\rm sub}/\delta M_{\rm clus} \sim (\sigma_{\rm sub}/\sigma_{\rm clus})^2$. Therefore, even the largest clumps of substructure with circular velocity ~300 km s$^{-1}$ will only produce fluctuations of order 5% in a rich, virialized, galaxy cluster. The global profiles may also vary from cluster to cluster, perhaps as a result of different formation histories.

The residuals from the best-fit NFW profiles to these halos show a characteristic S-shape with deviations of order 20%. Within 10% of the virial radius, a power law $\sim r^{-1.4}$ is an excellent fit. A simple modification to the NFW profile from $\rho(R) \propto [R(1+R^2)]^{-1}$ to $\rho(R) \propto [R^{1.4}(1+R^{1.4})]^{-1}$ fits our high-resolution simulations very well. (Here $R$ is the radius from the cluster center expressed in terms of the virial radius divided by a scale factor that is equal to $r_{\rm vir} \times 0.18$ for the halos simulated here). We emphasize the need to perform many more halo simulations at this resolution to study the scatter in the inner and outer slopes and the concentration parameter.

## 4. ACHIEVING CONVERGENCE IN HALO PROPERTIES: WHAT IS GOING ON?

What are the possible numerical or physical reasons behind the shape of CDM density profiles and the dependence upon resolution that we have investigated here?

The simplest interpretation is that the gravitational softening is affecting our results on scales less than about 4 or 5 softening lengths; all of the halo density profiles we have calculated agree very well beyond this scale. Thus, at our highest resolution we have converged upon a unique solution, and we can resolve the density profiles to ~1% of $R_{\rm vir}$ with $10^6$ particles and softening 0.2% $R_{\rm vir}$. However, we have demonstrated that changing the softening while keeping the mass resolution fixed leads to agreement between profiles on scales just larger than one softening length.

Splinter, Melott, & Shandarin (1998 and references therein) emphasize that many statistics are not accurately reproduced using $N$-body codes that are intrinsically collisional. In comparison with particle mesh codes, they argue that only scales larger than the mean interparticle separation should be considered. This would correspond to a scale about 10% of $r_{\rm vir}$ within our highest resolution simulation—an order of magnitude larger than our convergence tests suggest.

Evans & Colett (1998) demonstrated that a density profile with a slope of $-4/3$ is a stable solution to the Fokker-Planck and the collisional Boltzmann equations. However, we note that the trend in Figure 2 is opposite that expected from collisional effects. Furthermore, we do not observe a significant inward energy transfer as expected from the Evans & Colett model.

The inner density profiles may hold clues as to the initial power spectrum. For example, Subramanian & Ostriker (1998) extended Bertschinger's (1985) self-similar solutions to the spherical collapse model to include angular momentum. They find that the slopes of the profiles are directly related to the degree of translational motion and the spectrum of density fluctuations.

Steeper profiles may arise from substructure halos that are

[4] Although not plotted here, values of the comoving softening below 5 kpc lead to visible signs of relaxation in the density profile—the central region begins to expand. This evidence for collisionality occurs for values of the softening smaller than 1/200 of the mean interparticle separation within the cosmological volume simulated and less than 1/20 of the mean interparticle separation within the virial radius.

transferring material at high phase-space density to the center of the cluster (Syer & White 1997). As we move to higher resolution, we can resolve structure collapsing at earlier redshifts. This material at the highest physical density invariably ends up at the center of the cluster by $z = 0$. Because it is denser, it is more robust to tidal disruption, and it therefore has the potential of carrying more mass to the central regions.

We demonstrate the latter effect by tracing back the particles that lie within the final virial radius to their positions at $z = 5$. Using our highest resolution simulation, we find that 14% of the total mass of the final halo has already collapsed within small halos at $z = 5$. This material ends up constituting 75% of the mass within $0.01r_{\rm vir}$. However, within our medium-resolution simulation of the same halo, we find that only 2% of the mass of the final halo has collapsed by $z = 5$, and this ends up making just 20% of the halo mass within $0.01r_{\rm vir}$. The lowest resolution simulation does not contain any virialized halos at $z = 5$.

The power spectrum of CDM-type models asymptotes toward a slope $n = -3$ and provides power on all scales relevant to cosmological simulations. Therefore, most of the material in the CDM universe must lie in collapsed virialized clumps at high redshifts. If the simulations had even better mass resolution, we would have expected to observe halos collapsing at much earlier epochs and at higher phase-space densities. This material would end up at the center of the final cluster, perhaps altering the density profiles from what we find at the current resolution.

## 5. SUMMARY

We have performed the highest resolution simulations of cold dark matter halos to date. Our force resolution is 0.2% of the virial radii, and mass resolution is such that we can resolve halos 1/50,000 of the mass of the final system. The wealth of substructure within the final systems is phenomenal. We can identify approximately 1500 halos within halos at the final time. Some of the halos within the cluster's virial radius contain their own substructure!

Both particle number and softening play a role in shaping the final density profiles; as we increase the resolution, the halo profiles become steeper and denser in the centers. With the same force softening but with 10 times as many particles, an individual halo will be roughly twice as dense at $0.01r_{\rm vir}$, and increasing the mass resolution by another order of magnitude leads to densities that are a further 50% higher at the same radius. Even with $3 \times 10^6$ particles per halo, we might not have converged upon a unique density profile for cold dark matter halos. Of order $10^6$ halo particles must be used in order to compare the dynamics of the inner few percent of the cluster mass distribution with observations.

Our convergence tests suggest that our highest resolution simulation can be used to determine the density profile to a scale just less than ~1% of the virial radius. At this point, the profile has reached an asymptotic slope of $r^{-1.4}$. It will be interesting to study the statistics of gravitational arcs within clusters using steeper density profiles (e.g., Bartelmann 1996). Since galaxy halos will have steeper profiles at a fixed scale length compared to the cluster-sized halos simulated here, the problem of reconciling cold dark matter halos with observations of galaxy rotation curves will be considerably exacerbated by these results (Moore 1994; Flores et al. 1994).

We would like to thank John Dubinski, Gus Evrard, Carlos Frenk, Neal Katz, Adrian Melott, Julio Navarro, and Simon White for stimulating discussions on halo formation. We also thank Neal Katz for helping set up and run the Virgo Cluster simulation and the referee for comments that helped clarify the paper. This research required a great deal of computational resources, and we are indebted to NASA's High Performance Computing and Communications program and the Virgo Consortium. Computations were performed on the Pittsburgh T3E and the UK CCC Origin 2000. B. M. is a Royal Society University Research Fellow, and F. G. is supported by the European Network grant "Galaxy Formation and Evolution."

## REFERENCES

Bartelmann, M. 1996, A&A, 313, 697
Bertschinger, E. 1985, ApJS, 58, 39
Carlberg, R. 1994, ApJ, 433, 468
Craig, M. 1997, Ph.D. thesis, Univ. California, Berkeley
Crone, M. M., Evrard, A. E., & Richstone, D. O. 1994, ApJ, 434, 402
Davis, M., Efstathiou, G., Frenk, C. S., & White, S. D. M. 1985, ApJ, 292, 371
Dubinski, J., & Carlberg, R. 1991, ApJ, 378, 496
Evans, W. N., & Collet, J. L. 1998, ApJ, submitted
Flores, R. A., & Primack, J. R. 1994, ApJ, 457, L5
Frenk, C. S., White, S. D. M., Davis, M., & Efstathiou, G. 1988, ApJ, 327, 507
Frenk, C. S., et al. 1998, in preparation
Ghigna, S., Moore, B., Governato, F., Lake, G., Quinn, T., & Stadel, J. 1998, MNRAS, submitted
Moore, B. 1994, Nature, 370, 620
Moore, B., Katz, N., & Lake, G. 1996, ApJ, 457, 455
Navarro, J. F., Frenk, C. S., & White, S. D. M. 1996, ApJ, 462, 563
Quinn, P. J., Salmon, J. K., & Zurek, W. H. 1986, Nature, 322, 329
Splinter, R. J., Melott, A. L., Shandarin, S. F., & Suto, Y. 1998, ApJ, 497, 38
Subramanian, K., & Ostriker, J. 1998, in preparation
Syer, D., & White, S. D. M. 1997, preprint (astro-ph 9611065)
Tormen, G., Bouchet, F. R., & White, S. D. M. 1996, MNRAS, 286, 865
Warren, S. W., Quinn, P. J., Salmon, J. K., & Zurek, H. W. 1992, ApJ, 399, 405

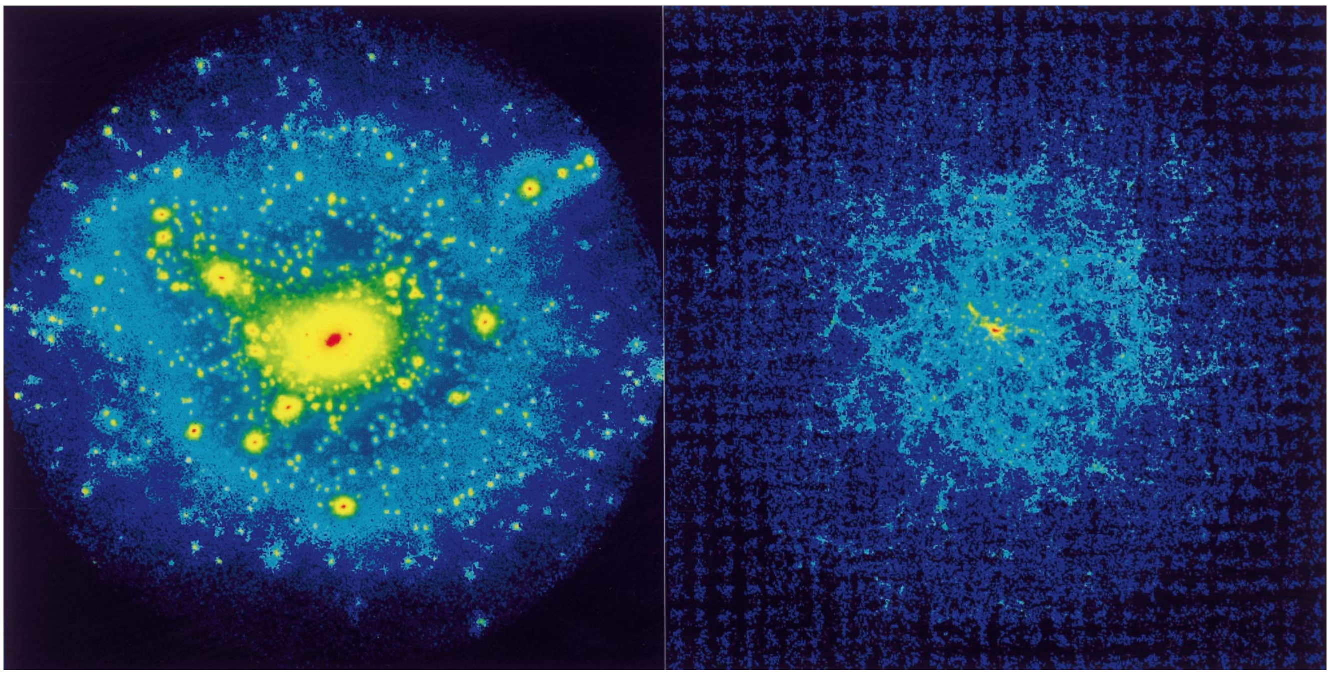

FIG. 1.—*Right:* A sphere of radius $r_{vir}$ that contains the cluster at $z = 0$. All of the visible halos and substructure in this plot lie within the virial radius. *Left:* Particle distribution in a 700 Mpc box from the resimulation of the Coma Cluster. This highlights the scale of the simulation and the seven refinement zones that focus in on the highest resolution region. The color scale in both panels represents the local overdensity at the position of each particle and reflects a variation from $10^1$ to $10^6$ times the mean density.

MOORE et al. (see 499, L6)

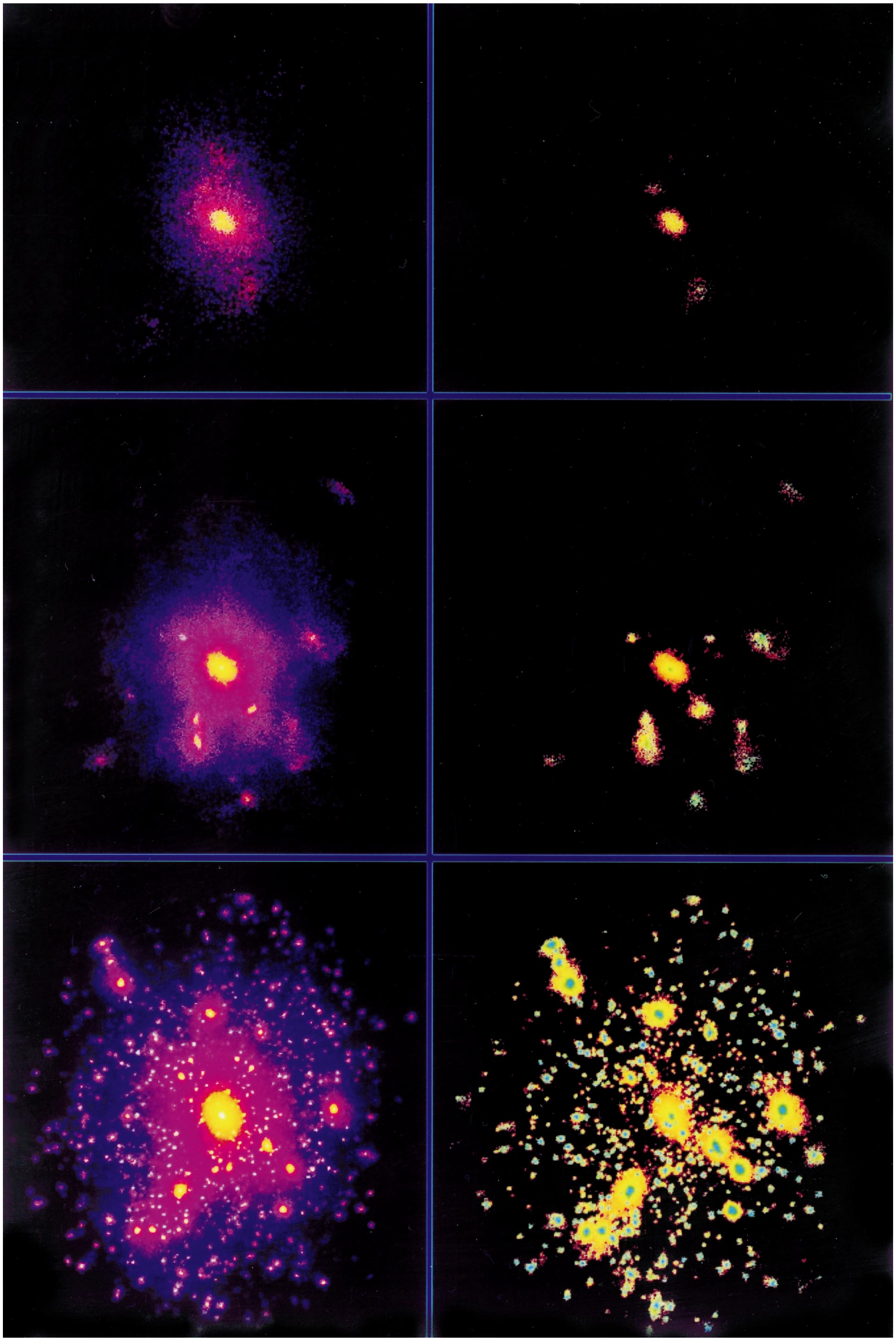

FIG. 2.—Projected particle distributions for the Coma Cluster at three different resolutions. In each case, we have extracted a sphere of radius equal to $r_{vir}$ = 3.4 Mpc. *Left:* Logarithm of the local density covering 5 orders of magnitude, from $\rho/\rho_0 = 10^1$ to $10^6$. *Right:* Local phase-space density $\rho/\sigma^3$, where $\sigma$ is the local velocity dispersion. These quantities are plotted at the position of each particle using a color scale spanning 5 orders of magnitude, and they are measured by smoothing over the nearest 64 particles.

MOORE et al. (see 499, L6)